Theoretical Analysis of ^{31}P NMR Chemical Shifts in Vanadium Phosphorus Oxides

V. Robert,*,†,‡ S. Petit,† S. A. Borshch,† and B. Bigot†

Institut de Recherches sur la Catalyse, UPR 5401, 2, avenue Albert Einstein, 69626 Villeurbanne Cedex, France, Ecole normale supérieure de Lyon, Laboratoire de Chimie Théorique, 46, allée d'Italie, 69364 Lyon Cedex 07, France, and Université Claude Bernard de Lyon I, 43, boulevard du 11 novembre 1918, 69622 Villeurbanne Cedex, France

Received: December 14, 1999; In Final Form: March 1, 2000

Our goal is to develop a theoretical methodology for the analysis of ^{31}P NMR spectra in vanadium phosphorus oxide (VPO) systems important in heterogeneous catalysis. Within the framework of density functional theory, we investigate the shielding of the phosphorus nucleus in a series of related compounds. The importance of the basis set is pointed out by looking at the influence of polarization functions on the chemical shift of phosphorus in H_3PO_4. Using the B3LYP functional, very good agreement with the experimental isotropic shielding is reached for the binuclear species $[(VO_2)_2(HPO_4)(2,2'\text{-bipy})_2]$ constructed from two edge-sharing dioxovanadium(V) octahedra. As a prime motivation, a parent vanadium(V) model of pyrophosphate catalyst is finally studied to compare ^{31}P numerical calculations with experiment. Satisfactory shielding constants are obtained, making phosphorus a probe to investigate the transition metal environment.

1. Introduction

Catalysts based on vanadium phosphorus oxides (VPO) are widely used for the industrial production of maleic anhydride from *n*-butane.[1,2] Vanadyl pyrophosphate, $(VO)_2P_2O_7$, is the main component of the active catalyst. However, it is widely accepted that other phases of VPO[3] are also involved in the catalytic reaction. Possible mechanisms of transformation between different phases during the reaction were proposed, but the exact nature of the catalytic active site has not been understood so far. It is quite natural that a large range of experimental methods (X-ray diffraction, EPR, IR-Raman spectroscopy, electrical conductivity, electron microscopy, etc.) has been used to analyze these systems. An important place in the experimental studies of VPO is occupied by NMR of ^{31}P and ^{51}V nuclei.[4−8] VPO phases that do not contain paramagnetic V^{4+} ions can be characterized by conventional magic angle spinning NMR spectroscopy, whereas in the presence of paramagnetic centers informative spectra can be obtained by the spin echo mapping technique.

The main findings for the different VPO systems obtained by NMR can be summarized as follows. Three different groups of signals can be identified around 0, 2300, and 4600 ppm, referred to as belonging to V^{5+}, V^{4+}, and V^{3+} phases, respectively. Within each group signals are spread over quite a large range, and in some cases an important temperature dependence is observed. The peaks positions depend on the local environment of phosphorus by vanadium atoms, and especially on the local V^{5+}/V^{4+} distribution, which in turn controls the maleic anhydride production.[1,2]

Recently, we analyzed a cluster model[9,10] of $(VO)_2P_2O_7$ in order to clarify the role of mixed-valence state ($V^{5+}-V^{4+}$) appearing under reaction. The layered structure is made of pairs of edge-sharing octahedra linked together by pyrophosphate $P_2O_7^{4-}$ units.[11] Along the [100] direction, V_2O_8 units are connected through V═O−V═O bonds in a distorted octahedral environment. We have shown that a minimal model describing valence states is given by two dimers along this direction. The stability of the corresponding four-nuclear vanadium cluster has been calculated against structural distortions appearing when the ratio V^{5+}/V^{4+} changes. Electron redistribution in this mixed-valence cluster turned out to be a driving force in the insertion mechanism of oxygen from the lattice vanadyl V═O group. However, this model did not contain explicitly any P atom and could not be used to study the NMR spectra. The complexity and richness of structural and electronic information contained in VPO NMR spectra ask for the development of new theoretical methodologies.

Ab initio calculations of NMR chemical shifts have been extensively developed for the past few years. Several reviews on this topic are available in the recent literature.[12,13] The ability to predict chemical shifts has undoubtedly strengthened the richness of this powerful spectroscopic technique. In that sense, different approaches were used to accurately estimate the shielding tensor and compare its isotropic part to experimental liquid NMR data. Excellent agreement with experiment (±0.1 ppm) for very small molecules with large basis sets was observed for proton shielding.[14,15] Pioneered calculations on phosphorus in PH_3[16] and in phosphine oxides were performed at Hartree−Fock and Møller−Plesset (MP2) theory levels with useful accuracy.[17] However, since long-distance electron correlation effects should be explicitly taken into account, these methods may not be well-adapted for larger systems. The use of large basis set is impractical to carry out elaborate calculations. Nonetheless, density functional theory (DFT) has emerged as an alternative approach to tackle systems of bigger size in a computationally inexpensive way.[18−23] Performances comparable to MP2 calculations were obtained for NMR shieldings and motivated the use of DFT methodology to push back the problematic limitation on the size of the molecules. The

* Author to whom correspondence should be addressed. E-mail: vrobert@ens-lyon.fr. Fax: (33) 4 72 44 53 99.

† Institut de Recherches sur la Catalyse and Laboratoire de Chimie Thérique.

‡ Université Claude Bernard de Lyon I.

10.1021/jp994400o CCC: $19.00
Published on Web 04/20/2000

calculations of ^{31}P chemical shifts were performed by the DFT methods for some simple molecules.[24,25] Although of greatest interest in defining local environment, calculations for phosphorus nucleus shifts have been extended only once to systems containing transition metals.[26] The presence and the nature of any metallic site can be identified from the interpretation of ^{31}P NMR spectra.

The calculations of ^{31}P chemical shifts in VPO or their models are limited by two important constraints. First, these are not molecular but extended solid-state systems. Calculations on model clusters definitely introduce an error, which is difficult to estimate. Second, V^{4+} is a paramagnetic ion (electronic configuration d^1), and in vanadyl pyrophosphate these ions are linked by exchange interactions, the scheme of which is still under discussion in the physical literature.[27] The conventional DFT methods have been mainly used (until now) for diamagnetic systems. It is well-known that the main contribution in NMR chemical shift is given by the hyperfine interaction.[28] Theoretical studies of NMR in magnetic exchange-coupled systems need not only quantum-chemical calculations of one-center hyperfine interactions but also consideration of the magnetic structure, which can be done on the basis of phenomenological Heisenberg−Dirac−Van Vleck Hamiltonian. This strategy was adopted for biological Fe−S clusters.[29]

Under these conditions, it is difficult to hope that quantum-chemical calculations can reproduce the chemical shifts of VPO with high precision. However, our goal, at least for this moment, is different. We would like to set up a method that could be used as a qualitative base to extract structural information from VPO NMR spectra. This method must be of comparable precision for simple molecules used as references in ^{31}P NMR spectroscopy and more complicated clusters containing several vanadium atoms. Thus, we decided to concentrate on small molecules containing phosphorus fragments of the system, namely, H_3PO_4 and $H_4P_2O_7$. Special care was taken with respect to the basis set and the role of polarization functions. The evaluation of the isotropic shielding constant in phosphoric acid was required since resonance of ^{31}P in H_3PO_4 is the reference standard for ^{31}P NMR. We then assessed our calculations on a binuclear vanadium complex containing the HPO_4^{2-} group as a bridge.[30] This structure is very similar to the one found in VPO. Finally, the four-center model previously constructed[9,10] was expanded in order to include phosphorus bridges. NMR calculations were performed on the diamagnetic 4-d^0 (four V(V)) electronic configuration. In the following, we provide details of the calculations we used along this approach to get a clearer understanding of the chemical shift variation in vanadium phosphorus oxide models.

2. Methodology

Various approaches for the calculations of chemical shifts have been used to solve the crucial gauge origin problem.[31,32] A survey of these developments is out of the scope of this paper. We rather focused on one specific method, namely, the GIAO procedure (Gauge Including Atomic Orbitals), as it already has a strong history of success.[33,34] We used the DFT/GIAO approach as implemented in the Gaussian 94 program.[35] We restricted ourselves to one single hybrid functional, namely, B3LYP, which proved its efficiency in structure optimization and NMR chemical shift calculations. All molecular systems studied in this paper were completely or partly optimized. As NMR calculations for elements such as phosphorus have received limited consideration, we paid special attention to the critical role of the basis set. The selection of a basis set will be considered in the next paragraph where phosphoric acid is studied.

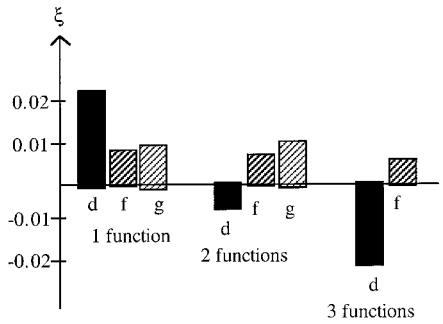

Figure 1. Chemical shielding of phosphorus in H_3PO_4 as a function of the nature and the number of polarization functions. The relative changes with respect to the reference calculation with the 6-311G basis are shown.

TABLE 1: Range of Shieldings of Phosphorus in Phosphoric Acid

basis set	description	shielding (ppm)
6-31G	double-ζ	366
6-311G	triple-ζ	295
D95	double-ζ	356
cc-pVDZ	double-ζ	393
cc-PVTZ	triple-ζ	313
cc-PVQZ	quadruple-ζ	333

3. Calculations of Phosphorus-Containing Molecular Systems

(a) Phosphoric Acid: A Reference Calculation. The ^{31}P NMR experimental reference is phosphoric acid 80% in water. The absolute chemical shielding value has been reported in the literature and given as 328 ppm.[36] The authors showed that accurate shieldings could be obtained if correlation and rovibrational corrections were included. Our goal was not to reproduce such a level of accuracy but rather to select a reliable enough basis set to perform all our calculations within the very same approach. Since much larger systems were to be investigated, we explored the possibility of getting satisfactory results with a modest amount of time. The comparison of density functional methods has been reported elsewhere and revealed that the GIAO/B3LYP procedure probably represents the best compromise.[20,37] Another motivation for the calculations of phosphoric acid is that it contains the PO_4 tetrahedral fragment, which is found in all VPO phases.

The molecule geometry was optimized under C_{3v}-symmetry constraint and standard 6-311G basis set. More extended bases do not lead to any meaningful geometrical changes. Table 1 summarizes the shielding constant values obtained from a selection of basis sets implemented in the Gaussian program.[35] According to our criteria, 6-311G turned out to be a satisfactory candidate. The corresponding shielding value σ(6-311G) = 295 ppm was chosen as an arbitrary reference calculation. One can then include very conveniently additional polarization and diffusion functions. As seen in Figure 1, the nature and the number of polarization functions play a dominant role in the calculation of chemical shielding constants. The geometry we determined with the 6-311G basis set was maintained in all these calculations. Thus, any variation in Figure 1 can be attributed to the size and the nature of the basis set. Let us clarify this important issue.

The picture we shall use is a one-electron excitation scheme.[38,39] First, let us briefly recall the theory of magnetic shielding to

get a clearer understanding of the changes we observed. Expression of the magnetic shielding of nuclei in molecules was first developed by N. F. Ramsey.[40] The electron−nucleus coupling in diamagnetic substances gives rise to energy modifications calculated by perturbation theory. Energy terms bilinear in the external field and the nucleus magnetic moment provide the contributions to the chemical shift tensor. The latter splits in two parts: the diamagnetic term Σ_d associated with the rotation of the ground-state cloud $|0\lambda\rangle$ and the paramagnetic one Σ_p resulting from the mixing of the ground state with excited states $|n\lambda\rangle$. The symbols we introduce here were defined in the original paper in which λ refers to the orientation of the molecule and $|n\rangle$ to the other degrees of freedom, namely, electronic and vibrational states. Following Abragam, the diamagnetic and paramagnetic tensors are decomposed into traceless parts $\Sigma'_d{}^{pq}$, $\Sigma'_p{}^{pq}$ and scalar ones σ_d, σ_p.[31] For our purposes, we concentrate on the scalar parts, independent of the index λ and written as

$$\sigma_d = \frac{e^2}{3mc^2}\left\{\left\langle 0\left|\sum_k \frac{1}{r_k}\right|0\right\rangle\right\} \quad (1)$$

$$\sigma_p = -\frac{2\beta^2}{3}\sum_{n\neq 0}\left\{\frac{1}{E_n - E_0}\langle 0|L|n\rangle\langle n|\sum_k l_k/r_k^3|0\rangle\right\} \quad (2)$$

As seen in eqs 1 and 2, the contribution of additional functions may be significant in the calculation of the tensor parameters. A clearer and not restrictive picture will arise from a two-electron system. Let us define φ_1 and φ_2 as the canonical spin orbitals. The ground-state wave function takes the usual form

$$|0\rangle = \begin{vmatrix}\varphi_1(1) & \varphi_2(1)\\ \varphi_1(2) & \varphi_2(2)\end{vmatrix} = |\varphi_1\varphi_2| \quad (3)$$

out of which a reference shielding value $\sigma = \sigma_d + \sigma_p$ is calculated.

If one increases the size of the basis set by including some polarization function χ_l, the net effect is the mixing of χ_l into φ_1 and φ_2. One should remember that a set of $(2l + 1)$ functions with $(-1)^l$ parity is actually added. χ_l can be associated to either the α or β spin part. Thus, we may write the new canonical functions as

$$|\tilde{\varphi}_1\rangle = N_1\{|\varphi_1\rangle + \alpha_1|\chi_l\rangle\} \quad \text{and} \quad |\tilde{\varphi}_2\rangle = N_2\{|\varphi_2\rangle + \alpha_2|\chi_l\rangle\} \quad (4)$$

and the perturbated ground state as

$$|\tilde{0}\rangle = |\tilde{\varphi}_1\tilde{\varphi}_2| = N_1N_2\{|0\rangle + \alpha_2|\varphi_1\chi_l| - \alpha_1|\varphi_2\chi_l|\} \quad (5)$$

N_1 and N_2 are normalizing factors. Using Slater's rules for the calculation of matrix elements, the scalar part of the diamagnetic tensor (see eq 1) becomes

$$\tilde{\sigma}_d = (N_1N_2)^2\{\sigma_d + |\alpha_1|^2\sigma_d^{(1)} + |\alpha_2|^2\sigma_d^{(2)}\}, \quad \text{where}$$
$$\sigma_d^{(i)} = \frac{e^2}{3mc^2}\left\langle \varphi_i\chi_l\left|\sum_k \frac{1}{r_k}\right|\varphi_i\chi_l\right\rangle \quad (6)$$

The number of nodes in the polarization function χ_l is greater than in φ_1 and φ_2. Thus its contribution close to the nucleus is reduced, and $\sigma_d \geq \sigma_d^{(i)}$. Since $N_i^2(1 + |\alpha_i|^2) = 1$, from eq 6, we get the following inequality

$$\tilde{\sigma}_d \leq \sigma_d \quad (7)$$

This result has a clear physical meaning. Additional orbitals create depletion of electronic density close to the nucleus. Thus, the hyperfine coupling is reduced by artificial electron density withdrawing. One should expect the very same trend for the paramagnetic component that is proportional to the expectation value of $1/r^3$. However, the smaller the potential range, the greater the changes in the electronic density in the vicinity of the nucleus. Therefore, the polarization function χ_l reduces to a larger extent the contribution of the paramagnetic shielding constant than the contribution of the diamagnetic one. As a result, the shielding constant is enhanced and $\xi = \{\tilde{\sigma} - \sigma(6\text{-}311G)\}/\{\sigma(6\text{-}311G)\} > 0$ as seen in Figure 1 (first series).

Even though the general behavior is the one expected from this elementary analysis, we felt that if one could clarify the contribution of polarization functions into electron circulation, a clearer control of the basis set size might result. Let us first point out the parity of the orbital momentum operator L. If Π stands for the parity operator,[41] then the X component L_X satisfies

$$\Pi L_x\Pi = \Pi(YP_Z - ZP_Y)\Pi = (-Y\Pi)(-\Pi P_Z) - (-Z\Pi)(-\Pi P_Y) = L_X \quad (8)$$

where we used the fact that position and momentum are odd operators. As expected, the orbital momentum operator is even. In the ground state $|0\rangle$, the second highest occupied molecular orbital (SHOMO) has main 3p-phosphorus character. In the presence of a polarization function χ_l, the ground state is $|\tilde{0}\rangle$ (see notation in eq 5) and the lowest unoccupied molecular orbital (LUMO) has main contribution on χ_l. From Slater's rules, nonzero matrix elements $\langle n|\sum_k l_k/r_k^3|0\rangle$, which are likely to contribute most to the paramagnetic part of the chemical shielding tensor, are proportional to $\langle 3p|\sum_k l_k/r_k^3|\chi_l\rangle$. Since $\sum_k l_k/r_k^3$ is an even operator, the matrix element is zero unless the two orbitals 3p and χ_l have identical parity. The conclusion we have just drawn out of the one-electron 3p $\leftrightarrow$ χ_l excitation is very similar to Laporte's rule. Thus, one should expect a larger reduction of the chemical shielding whenever odd functions are included. As seen in Figure 1, σ is smallest for f-type ($l = 3$) polarization functions.

The strong reduction of shielding with l character of polarization orbitals (d and g) is to be interpreted from the competition between the diamagnetic and paramagnetic contributions. As mentioned before, $\xi > 0$ along the first series. However, the most significant change in the paramagnetic shielding when one modifies the nature of the polarization function χ_l lies in the 3p $\leftrightarrow$ χ_l excitation term. Since the latter is zero (l is even, $l = 2$ and 4), shielding variations arise from perturbation of the diamagnetic part. The higher the orbital number l, the more diffuse the orbital. Therefore, the electron density in the vicinity of the resonant nucleus is reduced, and the diamagnetic shielding decreases. As seen in Figure 1, ξ is reduced when χ_l evolves from d to g-type.

As soon as another set of polarization functions χ'_l is added, the shielding decreases as a consequence of two dominant contributions. The paramagnetic part is hardly changed since 3p $\leftrightarrow$ χ'_l excitations are forbidden for $l = 2$. On the other hand, the diamagnetic shielding decreases from electronic density depletion, and a global decrease results. The trend is the one observed in Figure 1 and is very sensitive to the nature of the polarization function. As a matter of fact, low-lying polarization orbitals (i.e., d orbitals) have a greater tendency to mix into the ground state than the higher in energy do (i.e., f and g orbitals). An examination of Figure 1 reveals the modest contribution of a second set of f or g orbitals.

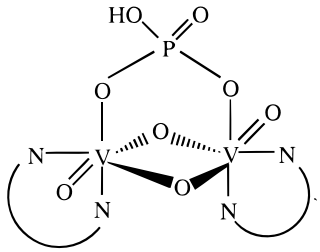

Figure 2. $[(VO_2)_2(HPO_4)(2,2'\text{-bipy})_2]$ molecule: a molecular system very similar to several VPO systems.

This preliminary approach sheds light on the very subtle participation of polarization functions. Special care should be taken when additional functions are artificially included. We have not detailed the changes in the ground state when self-consistency is achieved in the calculation. We believe that the most important contribution arises from the selection rule we identified.

(b) Diphosphoric Acid: A Comparative Calculation. Following the considerations presented above, 6-311G(d,p) was selected as the basis set in order to minimize the dependence of our calculations on numerical treatment. Using the isotropic chemical shielding constant of phosphoric acid as a reference, we were able to evaluate the isotropic chemical shift δ_{nuc} of any nucleus as

$$\delta_{nuc} = \frac{\sigma_{H_3PO_4} - \sigma_{nuc}}{1 - \sigma_{H_3PO_4}} \tag{9}$$

Our motivation was first to look into several phosphorus compounds to assess the numerical approach. In this respect, diphosphoric acid looked like a very important candidate since it contains a bitetrahedral species that takes part in the constitution of V^{4+} vanadyl pyrophosphate phases. The initial step was to fully optimize the geometry in which phosphorus atoms turned out to be strictly equivalent. For the optimized geometry, a -1.5 ppm chemical shift was found, reflecting the expected similarity between the electronic environments of phosphorus in H_3PO_4 and $H_4P_2O_7$. The chemical shift we calculated is also in good agreement with experimental data for $Na_4P_2O_7$ and $K_4P_2O_7$ reported in the literature, -1.6 and 2.5 ppm, respectively.[42]

These results suggested that our calculations were reliable enough to look into the chemical shift of systems including transition metals such as vanadium. As we were concerned with solid-state systems modeling, polynuclear complexes of vanadium were of special interest for us.

(c) A Molecular Model: $[(VO_2)_2(HPO_4)(2,2'\text{-bipy})_2]$. Since solid-state VPO systems were our principal preoccupation, we focused on a molecular architecture (see Figure 2) that is very similar to the building blocks in the different VPO phases. The diamagnetic V(V) molecule has been synthezied by J. Zubieta et al.[30] The structure consists of a binuclear neutral dioxovanadium complex. The vanadium sites exhibit highly distorted octahedral geometry defined by three oxo groups, the nitrogen donors of the chelating bipyridyl ligand and an oxygen donor of the η^2-bridging HPO_4^{2-} group. The $[VO(\mu_2\text{-}O)]_2^{2+}$ unit is nearly planar with the planes of bipyridyl ligands at right angles. Its configuration can be defined as *anti*-coplanar, whereas in VPO it is *anti*-orthogonal. The HPO_4^{2-} ligand caps the vanadium oxide rhombus and makes the system an ideal probe to investigate ^{31}P NMR in VPO. The crystallographic structure of $[(VO_2)_2(HPO_4)(2,2'\text{-bipy})_2]$ is known.[30] Optimization was limited to the bridging HPO_4^{2-} fragment, which was assumed to influence most the ^{31}P NMR signal.

TABLE 2: Shielding Tensor Elements of the $[(VO_2)_2(HPO_4)(2,2'\text{-bipy})_2]$ Molecule

δ_P	$\Delta\sigma$	η
9.7[a]	0.80[a]	31[a]
10[b]	0.02[b]	100[b]

[a] Simulated values from the experimental spectrum.[45] [b] Calculated values.

Following Chestnut's approach, we decided to describe the resonant nucleus environment at a high enough level of accuracy.[43] Therefore we stuck to the 6-311G(d,p) basis set for the HPO_4^{2-} fragment. Conversely, the extension of the basis was limited to 6-311G for the rest of the molecule. We assumed that the corrections arising from basis set modifications should be minor with respect to the local character of NMR spectroscopy. In the framework of these approximations, we determined the chemical shift as well as the shielding tensor parameters, namely, the anisotropy $\Delta\sigma$ and the asymmetry η defined as

$$\Delta\sigma = \sigma_{33} - (\sigma_{22} + \sigma_{11})/2$$

$$\eta = (\sigma_{22} - \sigma_{11})/(\sigma_{33} - \bar{\sigma}) \quad \text{and} \quad \bar{\sigma} = 1/3(\sigma_{33} + \sigma_{22} + \sigma_{11}) \tag{10}$$

Table 2 summarizes the calculations that were performed using the geometry optimized under the constraints defined above. The tensor elements were compared to the values obtained by computer simulation of the experimental spectrum.[44] They are given in Table 2 as well. As can be seen, satisfactory agreement is reached for the chemical shift. However, the asymmetry is strongly underestimated. The determination of the principal components of the tensor was reported to be a critical issue.[45] However, if one looks carefully at the molecule geometry, the experimental structure displays single and double P$-$O distances almost identical (1.55 and 1.51 Å, respectively). The presence of this local quasi-C_2-symmetry results in two very close principal components perpendicular to the symmetry axis. Indeed, the anisotropy increased as soon as the relative P$-$O distances values were modified on purpose. In fact, the studied complex crystallizes with one water molecule as $[(VO_2)_2(HPO_4)(2,2'\text{-bipy})_2]\cdot H_2O$. We believe that the presence of this water molecule amplifies the local asymmetry and might be responsible for such a large $\Delta\sigma$ value. It is well-known from silica studies that protonation is a key factor in the control of the tensor asymmetry.[46] Some complementary experiments on a dehydrated sample in connection with theoretical calculations that may include the water molecule are now under progress.

We were also concerned with the chemical shift dependence on the vanadyl group V$=$O distances. Both experimental and theoretical studies showed that the oxidation states of vanadium atoms in VPO are very sensitive to V$=$O distances.[9,10] In the catalysts, the V$=$O bonds are perpendicular to the $[V(\mu_2\text{-}O)]_2$ plane, whereas in the present molecular system they are coplanar. We did not observe any significant (more than 1%) change in the chemical shift when vanadyl distances were varied. Conversely, when one modifies the distances between the vanadium and the HPO_4^{2-} bridging group oxygen, the chemical shift changes by several parts per million. These results suggest that the electronic density in both the molecule and the catalyst is directly controlled by one category of V$-$O distances, namely, the ones perpendicular to the $[V(\mu_2\text{-}O)]_2$ plane.

(d) Cluster Model for Vanadyl Pyrophosphate. Following the type of description we used so far, we finally turned to a

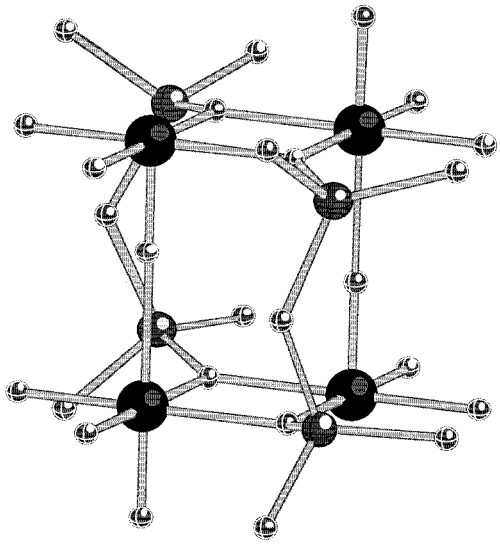

Figure 3. Four-nuclear vanadium cluster used as a model of VPO systems. The cluster is diamagnetic with vanadium oxidation state +V.

molecular model system for the VPO catalyst. The model we used was described previously and gave satisfactory interpretations of the importance of electron transfer in $(VO)_2P_2O_7$.[9,10] The layered structure of the catalyst was modeled by taking into account two $[V_2O_6]$ units connected through V−O bonds (see Figure 3). Different oxidation states for vanadium atoms were considered, and we showed that the electron trapping is directly controlled by the vanadyl V═O bond distances. Within this approach, the valence distribution $3V^{4+}$ (electronic configuration d^1)−$1V^{5+}$ (electronic configuration d^0) is consistent with the presence of approximately 20% of V(V) in the catalyst. However, in the present study we focused on one single valence state, namely, $4V^{5+}$. It should be noted that some proposed catalytic reaction mechanisms assume the formation of V(V) phases islets on the $(VO)_2P_2O_7$ surface. Structures containing edge-sharing VO_6 octahedra are also found in several V(V) phases, but with different links through PO_4 tetrahedra. Besides, let us recall that quantum-chemical calculations of the shielding tensor have been limited to diamagnetic species thus far. We intend to present the studies of paramagnetic configurations on the basis of a model Hamiltonian in future publications.

Phosphorus was explicitly added to our previous model through two pyrophosphate P_2O_7 bridges, resulting in a P/V = 1 as experimentally observed. Two symmetric bridges were taken, whereas in the real structure adjacent vanadium dimers are connected by only one. The dangling bonds were saturated by protons. The model cluster $[(VO)_2(\mu_2\text{-}O)_4(OH)_8(H_4P_2O_5)_2]^{4+}$ represented in Figure 3 was then partly optimized. The geometry optimization was indeed limited to the bridging $H_4P_2O_5$ moieties. Phosphorus atoms turned out to be approximately located in the $[V(\mu_2\text{-}O)]_2$ planes, which in our model are parallel to the catalyst surface. Optimized P−O distances were found around 1.56 Å. Since all phosphorus nuclei are structurally equivalent, one can expect a single NMR signal.

Chemical shift calculations were finally performed on the optimized structure. Our calculations showed that the phosphorus nucleus is deshielded by 60 ppm. This value falls in the range where experimentalists agree on the presence of V(V). In particular, the peak in pure V(V) solid $VOPO_4$ appears at 0 ppm, and the signal of phosporus bonded to V^{5+} species in strong interaction with $VO(PO_3)_2$ structure is shifted to −150 ppm.[5] We looked for a correlation between the chemical shift and the changes in the Mulliken charge on phosphorus. A decrease of 0.6 e^- is observed on phosphorus in comparison with diphosphoric acid, which contains a similar pyrophosphate group. It is quite natural that this electronic depletion leads to a significant deshielding of phosphorus nucleus. We found that this model system was able to reproduce with satisfactory accuracy the chemical shift values that have been determined experimentally. This is the first step in the calculation of ^{31}P NMR characteristics of such an important class of solids as VPO.

3. Conclusion

Using the GIAO method for the determination of chemical shielding tensor, we were able to investigate ^{31}P solid-state NMR in a series of phosphorus compounds. The nature of the basis set, and especially the number of polarization functions, was shown to be a critical issue. If agreement with experiment is to be reached, the basis set should be calibrated as an initial step. However, if one is rather interested in the trend of chemical shifts, a very standard basis set for phosphorus gives rise to satisfactory results. The presence of transition metal such as vanadium V(V) considerably modifies the calculated chemical shift. Depending on the number of metallic sites, deshielding values varying from 10 to 60 ppm were calculated. We were also able to demonstrate the very high sensitivity of vanadium oxides to bond distances perpendicular to the surface catalyst. Further efforts should be concentrated on the analysis of more detailed models for different VPO phases. In the near future, we intend to complete the description of VPO by taking into account paramagnetic centers. Studies based on the Heisenberg Hamiltonian are now in progress in our group.

Acknowledgment. We are grateful to Prof. J. Zubieta for providing us with the sample of the $[(VO_2)_2(HPO_4)(2,2'\text{-bipy})_2]\cdot H_2O$ compound and to S. Caldarelli for performing the NMR measurements on this sample and numerous discussions. We thank A. Tuel, J.-C. Volta, and V. Malkin for useful discussions related to this work.

References and Notes

(1) Special issue: Forum on Vanadyl Pyrophosphate Catalysts. Centi, G., Ed. *Catal. Today* **1993**, *16*, 1−147 and references therein.
(2) Trifiro, F.; Centi, G.; Ebner, J. R.; Franchetti, V. M. *Chem. Rev.* **1988**, *88*, 55 and references therein.
(3) Bordes, E. *Catal. Today* **1987**, *1*, 499.
(4) Li, J.; Lashier, M. E.; Schrader, G. L.; Gerstein B. B. *Appl. Catal.* **1991**, *73*, 83.
(5) Sananes, M. T.; Tuel, A.; Volta, J.-C. *J. Catal.* **1994**, *145*, 251.
(6) Sananes, M. T.; Tuel, A.; Hutchings, G. J.; Volta, J.-C. *J. Catal.* **1994**, *148*, 395.
(7) Sananes, M. T.; Tuel, A. *Solid State Nucl. Magn. Reson.* **1996**, *6*, 157.
(8) Vedrine, J.-C.; Millet, J.-M.; Volta, J.-C. *Faraday Discuss. Chem. Soc.* **1989**, *87*, 207.
(9) Robert, V.; Borshch, S. A.; Bigot, B. *Chem. Phys.* **1996**, *210*, 401.
(10) Robert, V.; Borshch, S. A.; Bigot, B. *J. Mol. Catal. A: Chemical* **1997**, *119*, 327.
(11) Gorbunova, Y. E.; Linde, S. A. *Sov. Phys. Dokl.* **1979**, *24*, 138.
(12) Chestnut, D. B. The Ab Initio Computation of Nuclear Magnetic Resonance Chemical Shielding. In *Annual Reports on NMR Spectroscopy*; Webb, G. A., Ed.; Academic Press: London, 1994; Vol. 29.
(13) Chestnut D. B. *The Ab Initio Computation of Nuclear Magnetic Resonance Chemical Shielding*; In Lipkowitz, K. B., Boyd, D. B., Eds. *Rev. Comput. Chem.* **1996**, *8*, 245.
(14) Chestnut, D. B. *Chem. Phys.* **1997**, *214*, 73.
(15) Sauer S. P. A.; Spirko, V.; Paidarova, I.; Kraemer, W. P. *Chem. Phys.* **1997**, *214*, 91.
(16) Wolinski, K.; Hsu, C. L.; Hinton, J. F.; Pulay, P. *J. Chem. Phys.* **1993**, *99*, 7819.
(17) Chestnut, D. B. *J. Am. Chem. Soc.* **1998**, *120*, 10504.
(18) Schreckenbach, G.; Ziegler, T. J. *J. Phys. Chem.* **1995**, *99*, 606.

(19) Rauhut, G.; Puyear, S.; Wolinski, K.; Pulay, P. *J. Phys. Chem.* **1996**, *100*, 6310.

(20) Cheesemann, J. R.; Trucks, G. W.; Keith, T. A.; Frisch, M. J. *J. Chem. Phys.* **1996**, *104*, 5497.

(21) Malkin, V. G.; Malkina, O. L.; Casida, M. E.; Salahub, D. R. *J. Am. Chem. Soc.* **1994**, *116*, 5898.

(22) Malkin, V. G.; Malkina, O. L.; Eriksonn, L. A.; Salahub, D. R. In *Modern Density Functional Theory: A Tool of Chemistry, Theoretical and Computational Chemistry*; Seminario, J. M., Politzer, P., Eds.; Elsevier: Amsterdam, 1995; Vol. 2, p 273.

(23) Bühl, M.; Kaupp, M.; Malkina, O. L.; Malkin, V. G. *J. Comput. Chem.* **1999**, *20*, 91.

(24) Kaupp, M. *Chem. Ber.* **1996**, *129*, 535.

(25) Ruiz-Moralez, Y.; Ziegler, T. *J. Phys. Chem. A* **1998**, *102*, 3970.

(26) Eichele, K.; Wasylishen, R. E.; Corrigan, J. F.; Taylor, N. J.; Carthy, A. J. *J. Am. Chem. Soc.* **1995**, *117*, 6961.

(27) Barnes, T.; Riera, J. *Phys. Rev. B* **1994**, *50*, 6817.

(28) Bertini, I.; Luchinat, C. *Coord. Chem. Rev.* **1996**, *150*, 1.

(29) Mouesca, J.-M.; Noodleman, L.; Case, D.; Lamotte, B. *Inorg. Chem.* **1995**, *34*, 4347.

(30) Zhang, J.; Haushalter, R. C.; Zubieta J. *Inorg. Chim. Acta* **1997**, *260*, 105.

(31) Abragam, A. *Principles of Nuclear Magnetic Resonance*; Oxford University Press: New York, 1961.

(32) Kutzlenigg, W.; Fleisher, U.; Schindler, M. The IGLO-Method: Ab Initio Calculation and Interpretation of NMR Chemical Shifts and Magnetic Susceptibilities. In *NMR, Basic Principles and Progress*; Diehl, P., Fluck, E., Günther, H., Kosfield, R., Seelig, J., Eds.; Springer-Verlag: Berlin, 1990; Vol. 23.

(33) London, F. *J. Phys. Radium* **1937**, *8*, 397.

(34) Ditchfield, R. *Mol. Phys.* **1974**, *27*, 789.

(35) Frisch, M. J.; Trucks, G. W.; Schlegel, H. B.; Gill, P. M. W.; Johnson, B. G.; Robb, M. A.; Cheeseman, J. R.; Keith, T.; Petersson, G. A.; Montgomery, J. A.; Raghavachari, K.; Al-Laham, M. A.; Zakrzewski, V. G.; Ortiz, J. V.; Foresman, J. B.; Peng, C. Y.; Ayala, P. Y.; Chen, W.; Wong, M. W.; Andres, J. L.; Replogle, E. S.; Gomperts, R.; Martin, R. L.; Fox, D. J.; Binkley, J. S.; DeFrees, D. J.; Baker, J.; Stewart, J. J. P.; Head-Gordon, M.; Gonzales, C.; Pople, J. A. *Gaussian 94*; Gaussian, Inc.: Pittsburgh PA, 1995.

(36) Jameson, C. J.; De Dios, A.; Jameson, A. K. *Chem. Phys. Lett.* **1990**, *167*, 575.

(37) Rablen, P. R.; Pearlman, S. A.; Finkbiner J. *J. Phys. Chem.* **1999**, *103*, 7357.

(38) *Multinuclear NMR*; Mason J., Ed.; Plenum Press: New York, 1987.

(39) Gilbert, T. M.; Ziegler T. *J. Phys. Chem.* **1999**, *103*, 7535.

(40) (a) Ramsey N. F. *Phys. Rev.* **1950**, *78*, 699. (b) Ramsey N. F. *Phys. Rev.* **1952**, *86*, 243.

(41) Cohen-Tannoudji, C.; Diu, B.; Laloë, F. *Mécanique Quantique*; Hermann: Paris, 1992.

(42) Duncan, T. M.; Douglas, D. C. *Chem. Phys.* **1984**, *87*, 339.

(43) Chestnut, D. B.; Byrd, E. F. C. *Chem. Phys.* **1996**, *213*, 153.

(44) Caldarelli, S. Private communication.

(45) Salzmann, R.; Kaupp, M.; McMahon, M. T.; Oldfield, E. *J. Am. Chem. Soc.* **1998**, *120*, 4771.

(46) Tuel, A. *Chem. Mater*. **1999**, *11*, 1865.